

Elastic Thickness Estimates for Venus Using Line of Sight Accelerations from Magellan Cycle 5

David N. Barnett, Francis Nimmo, and Dan McKenzie

Bullard Laboratories of the Department of Earth Sciences, University of Cambridge, Madingley Road, Cambridge CB3 0EZ, United Kingdom
E-mail: barnett@esc.cam.ac.uk

Received September 8, 1998; revised November 1, 1999

The elastic thickness, T_e , for various regions of Venus is estimated by comparing the observed line of sight (LOS) acceleration of the Magellan spacecraft with that predicted using a spherical harmonic representation of the topography, to degree and order 360. At long wavelengths (typically longer than about 500 km) the transfer function between the topography and gravity, or admittance, usually has a flat spectrum with a magnitude of between 20 and 50 mGal Km^{-1} , which is most likely due to convective support. In particular, the topographic highs associated with Beta, Phoebe, Bell, and Eistla are thought to be dynamically supported. At shorter wavelengths, the admittance increases, suggesting a component of flexural support. The elastic thicknesses are constrained by fitting theoretical admittance curves to the observed short wavelength values for the admittance. Results from Magellan cycle 5 show evidence of regional variations in elastic thickness between about 19 and 29 km, with a mean value of around 21–23 km, assuming a crustal thickness of 16 km and a density of 2670 kg m^{-3} . The observed variations in admittance between different regions are unlikely to be due to differences in crustal thickness or density, and probably represent real variations in T_e . The values obtained are similar to those from an identical analysis using cycle 4 data. Estimates of the elastic thickness of the Ovda and Alpha regions are unreliable, probably because the topography is not well determined. No reliable estimates of elastic thickness could be made from cycle 6 data where the altitude of the spacecraft was higher than about 300 km, due to the reduction in short wavelength signal amplitude with altitude. © 2000 Academic Press

Key Words: Venus; elastic thickness; admittance; gravity; line of sight acceleration.

1. INTRODUCTION

The elastic thickness, T_e , is the effective thickness of that part of the lithosphere which can support elastic stresses over geological time scales. Any load on the lithosphere can, in general, be expressed as a Fourier series of different wavelength loads. In the Fourier domain, the admittance, $Z(k)$, is the ratio between the gravity anomaly, $\Delta\bar{g}(k)$, caused by a topographic load on an elastic plate and the magnitude of the topography, $\bar{h}(k)$,

$$\Delta\bar{g}(k) = Z(k)\bar{h}(k), \quad (1)$$

where $k = 2\pi/\lambda$ is the wavenumber. The admittance depends on the elastic thickness and can be viewed as a filter which predicts the gravity anomaly given the topography, i.e., is the transfer function between gravity and topography (see McKenzie and Bowin 1976). The admittance is given by

$$Z = \frac{3g_0(\rho_c - \rho_w)}{2a\rho_p} \exp(-kz) \times \left[1 - \exp(-kt_c) / \left(1 + \frac{ET_e^3 k^4}{12(1 - \sigma^2)(\rho_m - \rho_c)g_0} \right) \right], \quad (2)$$

where g_0 is the mean gravity field (8.86 m s^{-2}), ρ_c is the crustal density (2670 kg m^{-3}), ρ_w is the density of the overlying fluid (0 kg m^{-3}), ρ_m is the density of the upper mantle (3300 kg m^{-3}), E is Young's modulus (10^{11} Pa) and σ is Poisson's ratio (0.25) for the elastic layer of thickness T_e , z is the height of the surface on which the gravity is measured above the mean upper surface of the elastic layer (i.e., the spacecraft altitude), t_c is the mean crustal thickness (16 km), a is the radius of the planet (6052 km), and ρ_p is the mean density of the planet (5200 kg m^{-3}). The implications of the chosen values for the crustal parameters are addressed under Discussion and Conclusions.

Admittance analysis uses free air gravity data. As the wavelength of a load tends to infinity (i.e., $k \rightarrow 0$), the load will be compensated for all values of T_e and thus produce no free air gravity anomaly. Hence at long wavelengths the admittance is zero. Conversely, at short wavelengths the admittance approaches a constant value, controlled by the density contrast between the load and the surrounding material. The wavelength at which a change between these two regimes is observed (i.e., where compensation ceases) is dependent on elastic thickness.

A further complication is that topography whose wavelength is longer than about 500 km may be dynamically supported by convection. Dynamically supported topography typically gives rise to an admittance spectrum which is flat at long wavelengths and has an amplitude of around 40–60 mGal km^{-1} in the absence of water (McKenzie 1994), depending on the lid thickness (Nimmo and McKenzie 1996). This characteristic convective signal is a joint contribution from the bulge in the surface, which

gives a positive gravity anomaly, and from the anomalously low density of the hot asthenospheric material underneath, which gives a negative, but smaller, anomaly. Note that the viscosity structure of the mantle will, in practice, determine the relative magnitudes of these two effects (see, e.g., Richards and Hager 1984, Ricard *et al.* 1984). Thus the admittance does not tend to zero at long wavelengths when the topography is convectively supported.

2. ADMITTANCE STUDIES OF VENUS FROM MAGELLAN DATA

For an elastic thickness of the order of 20 km, the change in the value of the admittance, from high values at short wavelengths to lower values at long wavelengths, occurs in the wavelength range 250–500 km. It is therefore this region which is of interest for determining T_e . One major problem with flexural signals in this wavelength range is that the coherent gravitational signals are attenuated as the orbital height, z , increases, by a factor of approximately $\exp(-2\pi z/\lambda)$. This attenuation means, for example, that a signal of wavelength 500 km will be attenuated by a factor of approximately $\exp(-6)$ ($\simeq 0.002$) at an orbital height of 500 km.

The topography of Venus is known and can be expressed in terms of spherical harmonics to degree and order 360 (Rappaport and Plaut 1999). This topographic model is an improvement over the previous one (Rappaport and Plaut 1994) because it includes corrections to the position of the spacecraft, derived from a recent high-resolution gravity model. The principal difference between the two is at wavelengths greater than 1000 km and therefore does not have an important influence on the admittance estimates at wavelengths shorter than 500 km. Initially, a value of 1 mGal km⁻¹ at all wavelengths is used to calculate the gravity potential. The three components of the gravity field at the altitude of the spacecraft can then be calculated, using the full spherical harmonic series to $l = m = 360$. The projection of these components onto the line of sight to the Earth is therefore the LOS acceleration which would be observed if the admittance were 1 mGal km⁻¹. The gravity field is obtained by measuring the acceleration of the spacecraft during its orbit along the line of sight (LOS) from Earth (see McKenzie and Nimmo 1997), by calculating the time derivative of the LOS velocity, v , every 4 s (Δt). The LOS acceleration, g_n , at each point is given by

$$g_n = \frac{v_{n+1} - v_{n-1}}{2\Delta t}, \quad (3)$$

which gives a properly centered value of the LOS acceleration at each time.

Equation (1) may then be used to find the admittance, $Z(k)$, between the observed and calculated LOS accelerations, by finding the transfer function between the calculated and observed LOS accelerations in the Fourier domain and by assuming that the calculated LOS acceleration is free from noise. Various sources of noise are discussed by McKenzie and Fairhead (1997) and

McKenzie and Nimmo (1997). On Earth, an important source of noise is subsurface density variations. On Venus, such variations are likely to be smaller, because sediments are absent and the crust is entirely volcanic. A more important source of noise is the signal propagation path from Venus to Earth. Because of variations in the electron density in the solar wind, the phase of the carrier frequency used to make Doppler measurements undergoes irregular variations which cannot be distinguished from the phase variations used to estimate the LOS accelerations. McKenzie and Nimmo (1997) showed that this solar wind noise increased rapidly when the path from Venus to Earth is close to the Sun (i.e., near superior conjunction). They used a simple model of electron density to describe the observed variations when the Earth–Sun–Venus angle, ψ , was greater than about 120°. At smaller values of ψ , they argued that the source of the noise was probably instrumental, since its magnitude is independent of ψ . Both the plasma and the instrumental noise increase with increasing frequency, and they are therefore easily recognized. In contrast, upward attenuation causes the true LOS acceleration from Venus to decay rapidly as the frequency increases (i.e., as the wavelength decreases).

As in McKenzie and Nimmo (1997), two-dimensional gridded boxes of the observed and calculated LOS accelerations were used in this work. The slow rotation of Venus causes the tracks to sweep gradually across the surface and the viewing angle changes slowly, allowing the data to be gridded before Fourier transforming. Better results are achieved with 2-D, rather than 1-D, Fourier transforms, because the instrumental and solar wind noise is confined to each track and therefore has a short wavelength normal to each track. Therefore this noise has higher values of k in 2-D than it does in 1-D. Multitapers (Thomson 1982) are used to window the data three times in each dimension, using orthogonal windows, before the 2-D Fourier transform is carried out. The multitaper method reduces spectral leakage and also reduces the standard deviation of the estimates of Z , because it gives nine independent estimates of the admittance for each wavenumber band.

The best method of determining the admittance depends, in general, on whether there is more noise in the observed gravity, g , or in the topography, h . Since the observed LOS gravity tends to be noisier than the topography, the admittance is calculated using

$$Z(k) = \frac{\sum g(k)h^*(k)}{\sum h(k)h^*(k)}, \quad (4)$$

where the summation is over some wavenumber band of width Δk centred on k , ($=(k_x^2 + k_y^2)^{1/2}$) (see McKenzie 1994). The asterisk denotes the complex conjugate. This method assumes that the admittance is isotropic and that the topography is free from noise. However, in practice there may be noise in the topography, which tends to reduce estimates of the admittance (McKenzie 1994). The topography is poorly determined in regions such as tesserae (highly deformed, elevated regions). In such regions of

rough topography, the radar returns that are used to map the surface topography come from a large region of surface below the spacecraft, and it is difficult to pick the first return because the signal is wrapped round in time by the pulse repetition frequency (see Ford *et al.* 1993, McKenzie and Nimmo 1997). Rough areas where the topography is poorly constrained show up brightly in the synthetic aperture radar (SAR) images. This problem means that the spherical harmonic representation of the topography, which is used to calculate the gravity, is not accurate in such regions.

Other methods which have been used to estimate elastic thickness include the modeling of topography in the space domain. Johnson and Sandwell (1994) modeled flexural features associated with coronae, using 2-D Cartesian and axisymmetric thin elastic plate models. They found elastic thicknesses in the range 12–34 km for the most reliable data. Brown and Grimm (1996) carried out a study of several large impact craters on Venus. They observed no evidence of post-impact elastic rebound in any of these craters, such as the presence of faulting in the floors of the craters. Their interpretation was that the lithosphere was sufficiently rigid to support the crater cavities, constraining the elastic thickness for the three largest craters to be at least 10–15 km. McGovern and Solomon (1998) constrained the elastic thickness by studying the mechanisms necessary for the growth and support of large venusian volcanoes. They concluded that large conical volcanoes are much more likely to form if T_e is relatively large, a value of at least 32 km being required to allow the formation of the largest 25% of volcanoes on Venus.

Other studies have estimated T_e using the admittance calculated directly from spherical harmonic models of the gravity and topography. Smrekar (1994) inverted the raw LOS accelerations, in addition to spherical harmonic models, to generate a gravity field which she used to estimate an elastic thickness for Atla of 30 ± 5 km. Phillips (1994) also used spherical harmonic representations of the gravity and topography, to determine the elastic thickness of Atla using a Monte Carlo inversion technique which found the best-fit value of T_e and three other parameters to the observed admittance spectrum. His best-fit value of elastic thickness was 45 ± 3 km, although any values of T_e from 0 to 140 km gave acceptable solutions. However, more recently, Phillips *et al.* (1997) have argued that an elastic thickness of 25 km provides a better fit to the data. In addition, Simons *et al.* (1997) developed a method for analyzing the frequency content of the spherical harmonic data as a function of position. They found that the long wavelength topography of Venus is dominated by convective features, the admittance spectra implying values of elastic thickness of between 10 and 30 km.

Spherical harmonics must be used rather than Fourier transforms when the size of the area under consideration is comparable to the radius of the planet. To produce a spherical harmonic representation of the gravity field from the LOS velocity data, some method must be used to suppress the instability that arises from downward continuation; otherwise the gravity field is dom-

inated by the short wavelength noise. It is therefore difficult to estimate T_e directly from spherical harmonic models of the gravity field unless the signal to noise ratio in the LOS acceleration is high between wavelengths of 300 and 500 km. This condition is only satisfied by the Magellan data that was obtained at the lowest altitudes. In contrast, the method described by McKenzie and Nimmo (1997) can provide reliable estimates of Z when the signal to noise ratio is as low as 1 to 100, provided the noise is not coherent with the topography. This condition is satisfied by instrumental and solar wind noise.

3. ANALYSIS OF MAGELLAN MAPPING CYCLES

Magellan cycles 5 and 6 followed the circularization of the spacecraft's orbit (see Saunders *et al.* 1992). Previously, the orbit had been highly elliptical and approximately polar, with a periapse at about 10°N . The altitude at periapse was about 180 km for cycle 4, and the apoapse distance was approximately 8000 km. In an analysis of this cycle by McKenzie and Nimmo (1997), no data was used when the altitude of the spacecraft was greater than 400 km, which restricted the analyses to a latitude band of 25°S to 40°N . Cycles 5 and 6 can potentially be used to study areas at higher latitudes than was previously possible (see Figs. 1–3).

In any admittance analysis of an area of Venus, there are two important criteria which must be satisfied. First, the altitude of the spacecraft must not be too high. As the altitude increases, the attenuation of the gravitational signals increases rapidly, with this effect being most pronounced for short wavelength signals. At a given altitude, there will be some wavelength below which the signal coherence is so low (typically below about 0.01) that the estimates of the admittance are unreliable. It is important that the altitude is sufficiently low that the short wavelength elastic signals are not too greatly attenuated; otherwise the theoretical admittance curve which is fitted to the points will not be constrained. A useful rule of thumb is that the height of the spacecraft must be less than the wavelength at which the flexural admittance decreases rapidly as the wavelength increases. In practice, the admittance technique was not able to give a reliable estimate of T_e for cycles 5 and 6 when the spacecraft altitude was greater than about 300 km.

The second important point is that the area studied must not be too small. A large box is necessary if there is to be enough information present to allow accurate estimates of the admittance from noisy data. Also, not only does a box smaller than about 40° , or 4000 km in either dimension, limit the signal wavelength which can be studied but also it may result in spectral leakage, where a real signal with a wavelength longer than the box size will be mapped onto shorter wavelengths.

In addition, it is important to use a map projection which minimizes length and angular distortion. For example, in the case of Mercator projection with an axis through the pole, features near the poles are stretched relative to those nearer the equator. In the case of boxes which extended more than about 45° or so

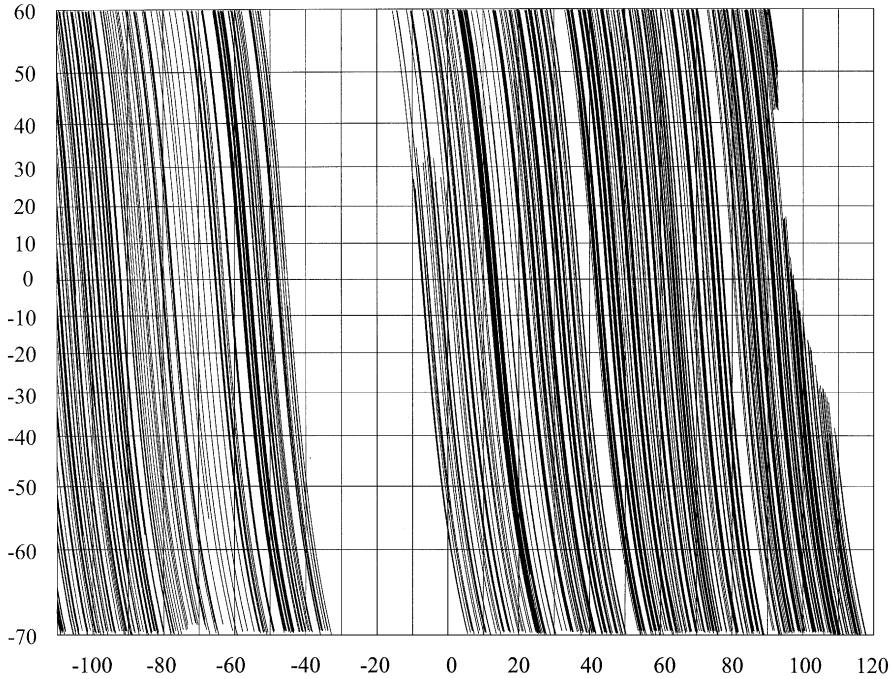


FIG. 1. Plot of the ground tracks of Magellan for which observed LOS accelerations are available, for cycle 5. Only those tracks where the altitude of the spacecraft was less than 400 km are shown. Ascending tracks which cut across these descending tracks are also not shown; the ascending tracks correspond to a different line of sight and therefore cannot be combined in the same admittance calculation.

in latitude, this stretching can be of order 1.5 or more. Studying large areas in such a Mercator projection can lead to errors in the calculated value of T_e of also about this order. In this work, an Airy projection (Snyder 1989) was used for all admittance

boxes, with a pole roughly in the center of the box in each case.

In order to reduce short wavelength gridding noise, the data (both observed and calculated LOS accelerations) were

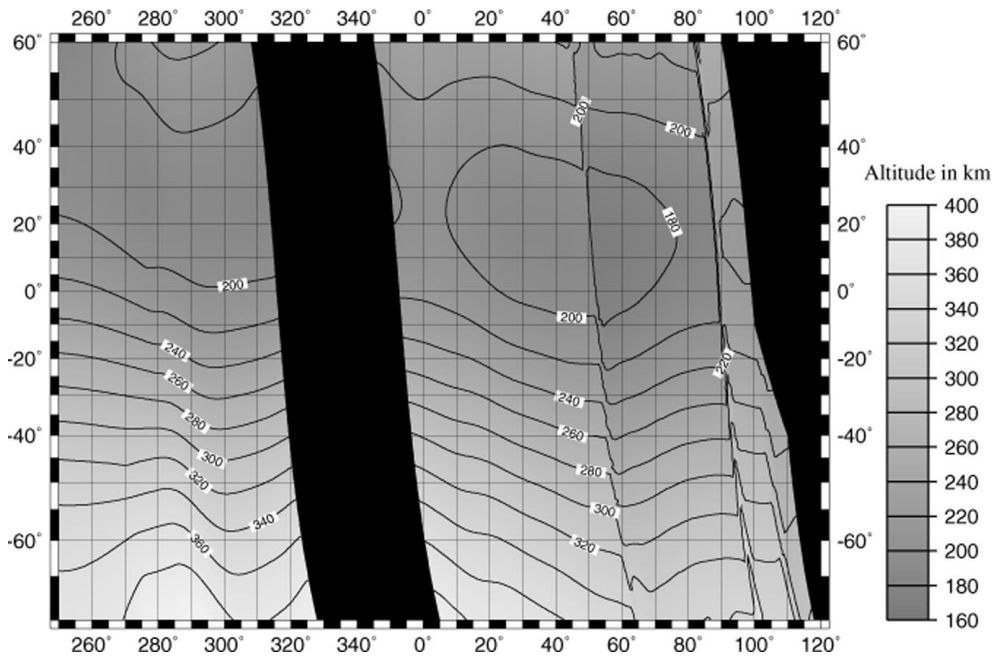


FIG. 2. The altitude of the spacecraft in km over the region where there is track coverage, for cycle 5. The black areas represent data gaps. The abrupt changes in altitude near 50°E and 90°E are due to maneuvers of the spacecraft (Konopliv and Sjogren 1996).

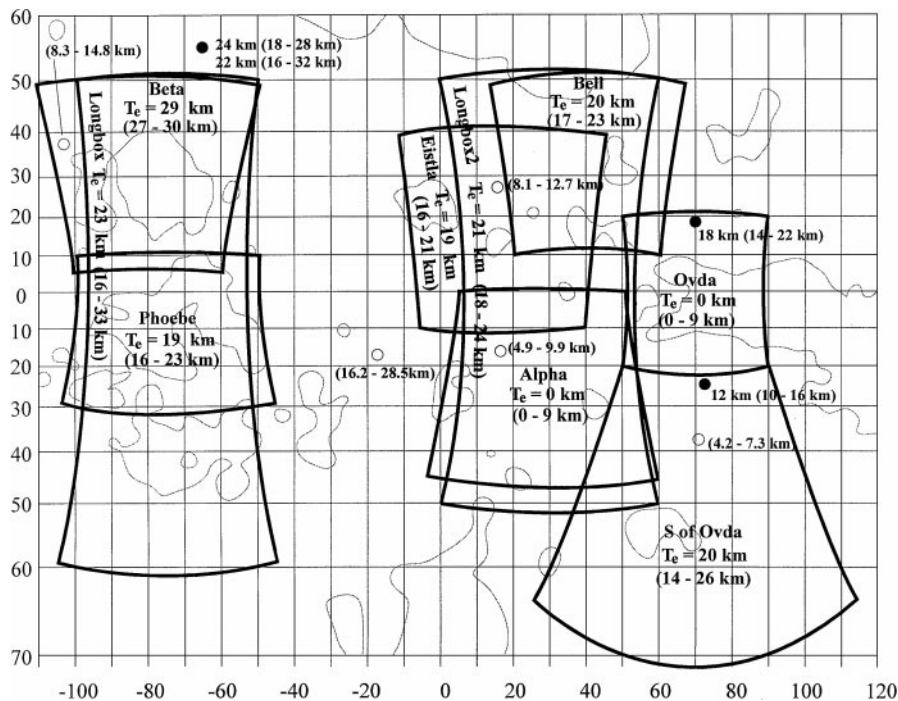


FIG. 3. The locations of the boxes used for the admittance studies with the cycle 5 data set and the best-fit elastic thicknesses. In each case, the range of elastic thickness over which the misfit function is less than twice that at its minimum is shown in brackets. Note that each box is rectangular in an Airy projection, but not in this Mercator projection. Also shown for comparison are local values of elastic thickness calculated by Johnson and Sandwell (1994) from the topography, using flexural models roughly perpendicular to strike of large features (filled circles) and smaller axisymmetric features (open circles). For each, the range of elastic thicknesses found are shown in brackets, and for the large features, the best-fit elastic thicknesses are also shown. The gray line is the 6052.5 km elevation contour.

smoothed before gridding. The smoothing was achieved by binning the data into $0.5^\circ \times 0.5^\circ$ bins and calculating the mean values of the locations and accelerations within each bin. Such bins are much smaller than the shortest wavelength which can be studied at the spacecraft altitude. The binning was necessary, as linear tracks of noise, roughly parallel to the track orientations, were visible when observed LOS acceleration was gridded without binning. This noise arose because the gridding code introduced large amplitude signals in locations where the tracks were closely spaced and adjacent values of LOS acceleration differed slightly, in an attempt to fit as many of the data points as possible. The observed and calculated accelerations must be smoothed in exactly the same way, because the smoothing window affects the amplitude at a particular wavelength.

One of the major aims of this work was to obtain estimates of elastic thickness, T_e , for different regions of Venus, and to see whether there are variations in this parameter over the planet. The reliability of these estimates, and hence the meaningfulness of any observed variations, may be ascertained both by the quality of the fit of the theoretical admittance curve to the points (shown by the misfit function, as defined by McKenzie and Fairhead (1997) and by comparison of the results with those from the cycle 4 data set (McKenzie and Nimmo 1997).

4. RESULTS FROM CYCLE 5

Figure 1 shows the ground track coverage for cycle 5 of that part of the surface of Venus over which the studies were carried out. Figure 2 shows the altitude of the spacecraft, as a function of position, and Fig. 3 shows the locations of the boxes used for the admittance studies which are discussed below. In Fig. 1, only tracks where the altitude of the spacecraft was less than 400 km are shown. Note that the coverage is not complete, both because there is no data from when the craft was occulted by Venus and near superior conjunction and because the signals from Magellan were not recorded continuously, even when the craft was not occulted. For each box studied, only tracks with a consistent orientation throughout the box were used, corresponding to a slowly varying LOS direction. It was important not to have two sets of tracks from different times, or from ascending and descending orbits, which have different viewing geometries, in the same box.

In the case of cycle 5, there were two main regions in which the spacecraft altitude was sufficiently low to allow T_e to be estimated. These were the two “longbox” regions (areas as shown in Fig. 3 and with approximate latitude and longitude limits as specified in Table I), in which the spacecraft altitude was between about 200 and 350 km. These were then subdivided into

TABLE I

Names and Approximate Latitude and Longitude Limits (for Cycle 5) of the Admittance Boxes, as Well as the Wavelength Bands in Which the Misfit Function Was Calculated, the Best-Fit Value of T_e (and the Range of Elastic Thickness over Which the Misfit Function Is Less Than Twice That at Its Minimum), and the Mean Spacecraft Altitude within Each Box

Region	Cycle	Lat. (°)	Long. (°)	λ band (misfit) (km)	Best-fit T_e (km)	Mean altit. (km)
“Longbox”	5	−60 to 50	−100 to −50	300 to 500	23 [16 to 33]	243
“Longbox2”	5	−50 to 50	0 to 60	300 to 500	21 [18 to 24]	226
Beta	5	5 to 50	−100 to −60	300 to 500	29 [27 to 30]	194
Phoebe	5	−30 to 10	−100 to −50	300 to 500	19 [16 to 23]	226
Bell	5	10 to 50	20 to 60	300 to 500	20 [17 to 23]	192
Eistla	5	−10 to 40	−5 to 40	350 to 500	19 [16 to 21]	198
S of Ovda	5	−70 to −20	50 to 90	300 to 500	20 [14 to 26]	281
Ovda	5	−20 to 20	50 to 90	300 to 500	(0 [0 to 9])	196
Alpha	5	−45 to 0	5 to 50	350 to 500	(0 [0 to 9])	239
Atla	4			150 to 500	32.5	
Ulfrun	4			150 to 500	33.0	
Phoebe & Beta	4			150 to 500	27.5	
Eistla	4			150 to 500	20.5	
Aphrodite	4			150 to 500	5.0	
Dali	4			150 to 500	12.0	

Note. The values of T_e for Ovda and Alpha are not likely to be valid. The elastic thickness estimates from cycle 4 are from McKenzie and Nimmo (1997).

smaller regions for study. Figure 2 also shows two abrupt jumps in the altitude of the spacecraft during cycle 5, near 50° and 90° longitude. These correspond to maneuvers of the spacecraft. The first was a lowering of the periaapse, and the second is due to a series of maneuvers which raised the periaapse and lowered the apoapse (Konopliv and Sjogren 1996). These maneuvers do not affect the observed LOS acceleration, provided the period in which the manoeuvre itself occurred is not used.

4.1. Beta

The region of Beta is discussed here as a representative example of the areas studied. The location of the box is shown in Fig. 3 and is specified in Table I by approximate latitude and longitude limits. The average altitude of the spacecraft within the box is also shown. A crustal thickness of 16 km and a density of 2670 kg m^{-3} were assumed for all regions (but see the discussion below). The best-fit elastic thickness for Beta is shown in Table I, and plots of the admittance, signal coherence, and misfit function of the admittance as a function of elastic thickness for the region are all shown in Fig. 4. The wavelength band in which the misfit function was calculated is also shown, and it is tabulated in Table I. It is important not to include long wavelengths where effects other than those due to elastic flexure dominate the admittance, and no data is used to constrain the theoretical curve until the admittance estimates show a marked increase from their long wavelength value (typically around 50 mGal km^{-1} .) The shorter wavelength limit is the wavelength below which the coherence is too low for the calculated admittance values to be reliable. However, the inclusion of shorter wavelengths in the misfit calculation does not affect the estimate of T_e , since the uncertainty in the admittance is large at short wave-

lengths, which therefore contributes little to the misfit function. The misfit function shows the amount by which the effective elastic thickness estimate can be varied without seriously degrading the quality of the fit to the data. The range of elastic thicknesses for which the misfit function is less than twice that at its minimum is also given, as a guide to the uncertainty. The shortest wavelength used by Simons *et al.* (1997) is shown in Fig. 4 by a vertical dashed line, and it is longer than the longest wavelength used in this work to estimate T_e . Figure 5 shows the theoretical admittance curves for the upper and lower T_e limits and the calculated admittance values. Shown for comparison is Eistla (see Table I), an area where T_e is less well constrained (see also Fig. 11).

At long wavelengths, the admittance spectrum is flat and has an amplitude of approximately 50 mGal km^{-1} (see Fig. 4). A flat, long wavelength spectrum of such a large amplitude is diagnostic of dynamic support (Simons *et al.* 1997), and the magnitude is consistent with models of mantle convection (Nimmo and McKenzie 1996, McKenzie 1994). Beta is therefore suspected to be convective in origin. In agreement with this conclusion is the fact that contour plots of observed and calculated LOS acceleration for Beta (Fig. 6) show that the dominant feature of the area is the positive topographic and gravity anomaly of Beta itself, with a diameter of around 2000 km. The evidence of rifting and volcanic constructs in the SAR images is also important. For these reasons, numerous previous studies have also concluded that Beta, and many of the other broad topographic rises on Venus, are associated with convective mantle plumes (e.g., Smrekar 1994, Phillips *et al.* 1981, McGill *et al.* 1981). Note that the contour interval for the calculated LOS acceleration plot is 50 times smaller than for the observed acceleration. Hence the similarity

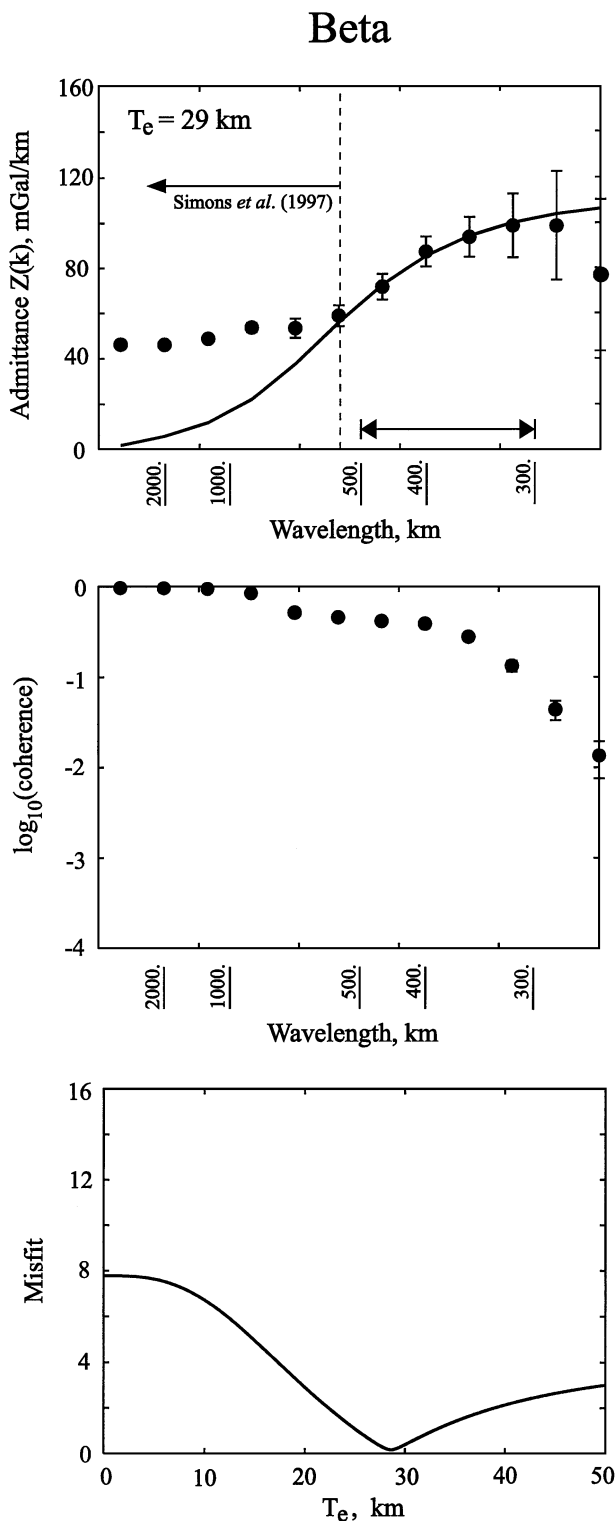


FIG. 4. Plots of admittance as a function of wavelength, signal coherence as a function of wavelength, and misfit function (to the data points) as a function of T_e , for the Beta region, using the box shown in Fig. 3. The minimum in the misfit function shows the best-fit T_e ; the wavelength band used is shown in Table I and by a double-headed arrow on the admittance plot. The vertical dashed line shows the wavelength corresponding to the value of l_{nyq} in the study by Simons *et al.* (1997) of the same region.

between the two plots in Fig. 6 is consistent with the fact that the long wavelength admittance is approximately 50 mGal km^{-1} .

The estimate of T_e for Beta (Fig. 4) is well constrained, because the altitude of the spacecraft is low and the gravity variations are large. Thus the admittance values down to wavelengths of around 300 km are reliable, despite the presence of noise in the observed LOS acceleration (see Fig. 6). The prolate spheroidal wavefunctions used as tapers are designed to avoid spectral leakage, which is anyway unlikely to be a problem when neither the topography nor the gravity has peaks. This argument was tested by prewhitening the calculated LOS acceleration with a suitable transfer function. As expected, this test showed that spectral leakage is unimportant when multitapers are used. The size of the error bars on the admittance estimates is related to the coherence between the observed and calculated LOS accelerations and the number of estimates in each wavenumber band (see McKenzie 1994). There is therefore a trade-off between Δk ,

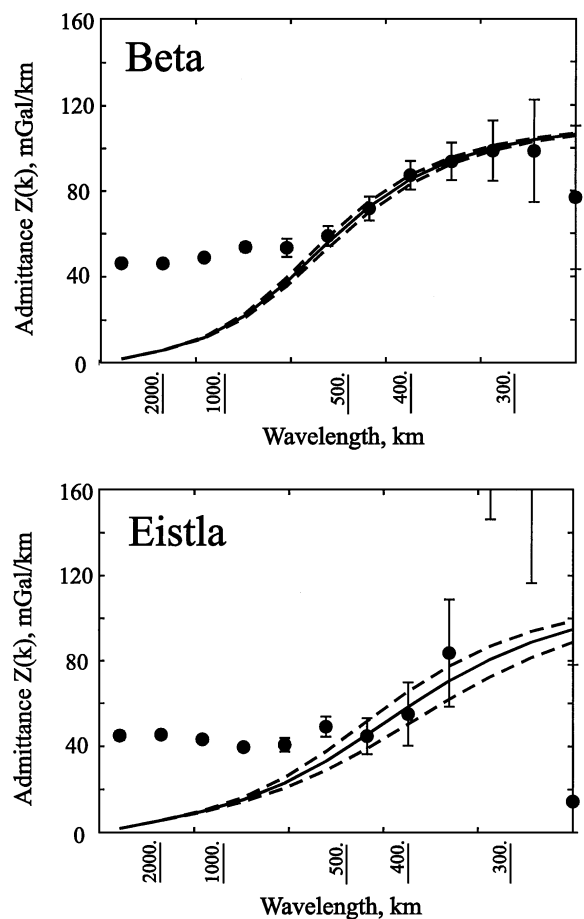
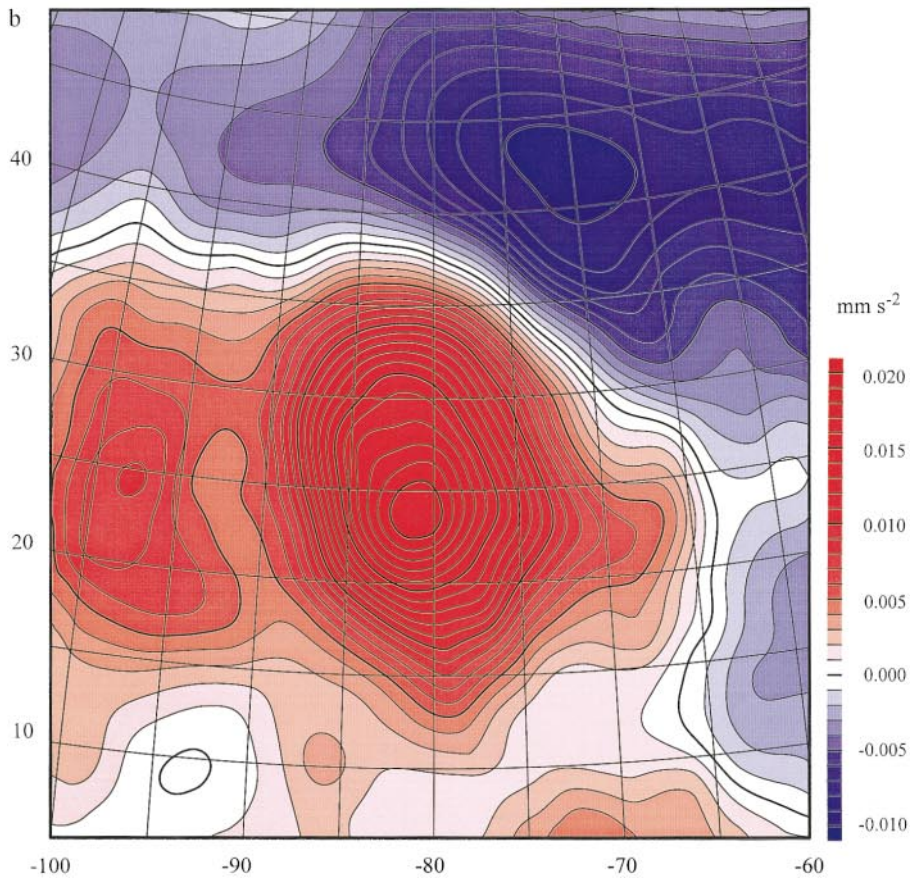
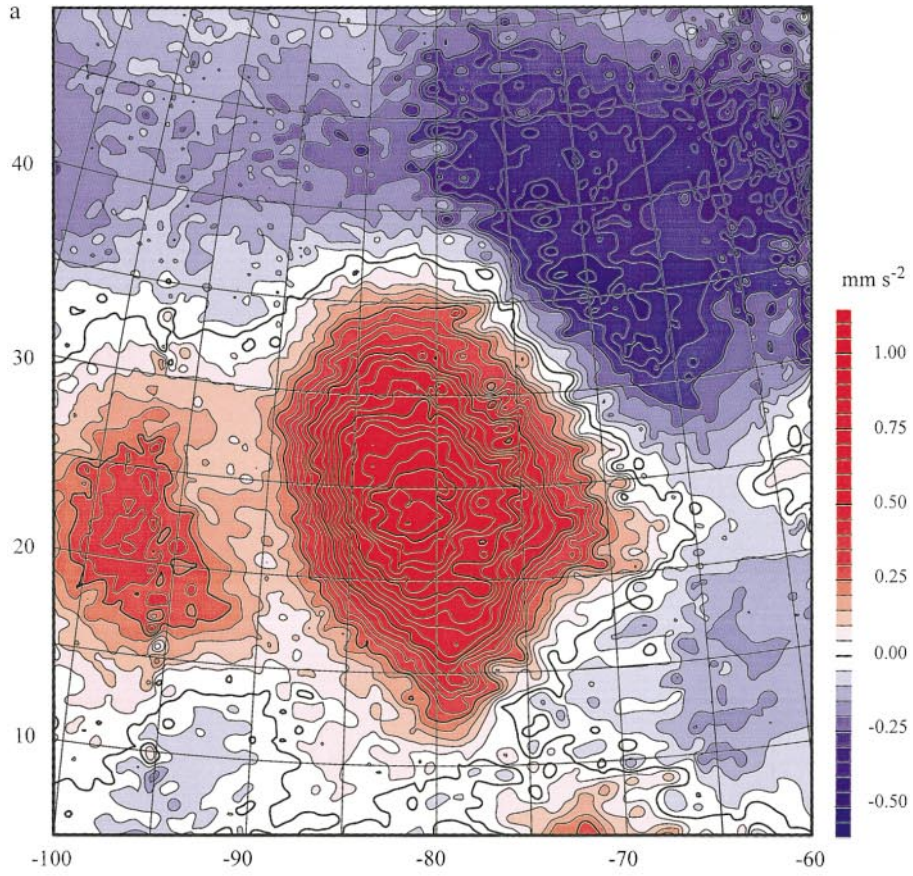


FIG. 5. Admittance plots for Beta and Eistla, as functions of wavelength. The theoretical curves for the best-fit elastic thicknesses (solid line) and for the upper and lower limits of elastic thickness within uncertainty (those elastic thicknesses for which the misfit function is twice that at its minimum), shown by dotted lines, are fitted to the data points in each case. The best-fit elastic thickness for Beta is 29 km, with an uncertainty range of 27–30 km, and the best-fit elastic thickness for Eistla is 19 km, with an uncertainty range of 16–21 km.

FIG. 6. Plots of observed (a) and calculated (b) LOS acceleration for the Beta region (cycle 5). The contour intervals are, respectively, 0.05 and 0.001 mm s^{-2} . The calculated LOS acceleration assumes an admittance at all wavelengths of 1 mGal km^{-1} and uses spherical harmonic topography to degree and order 360.



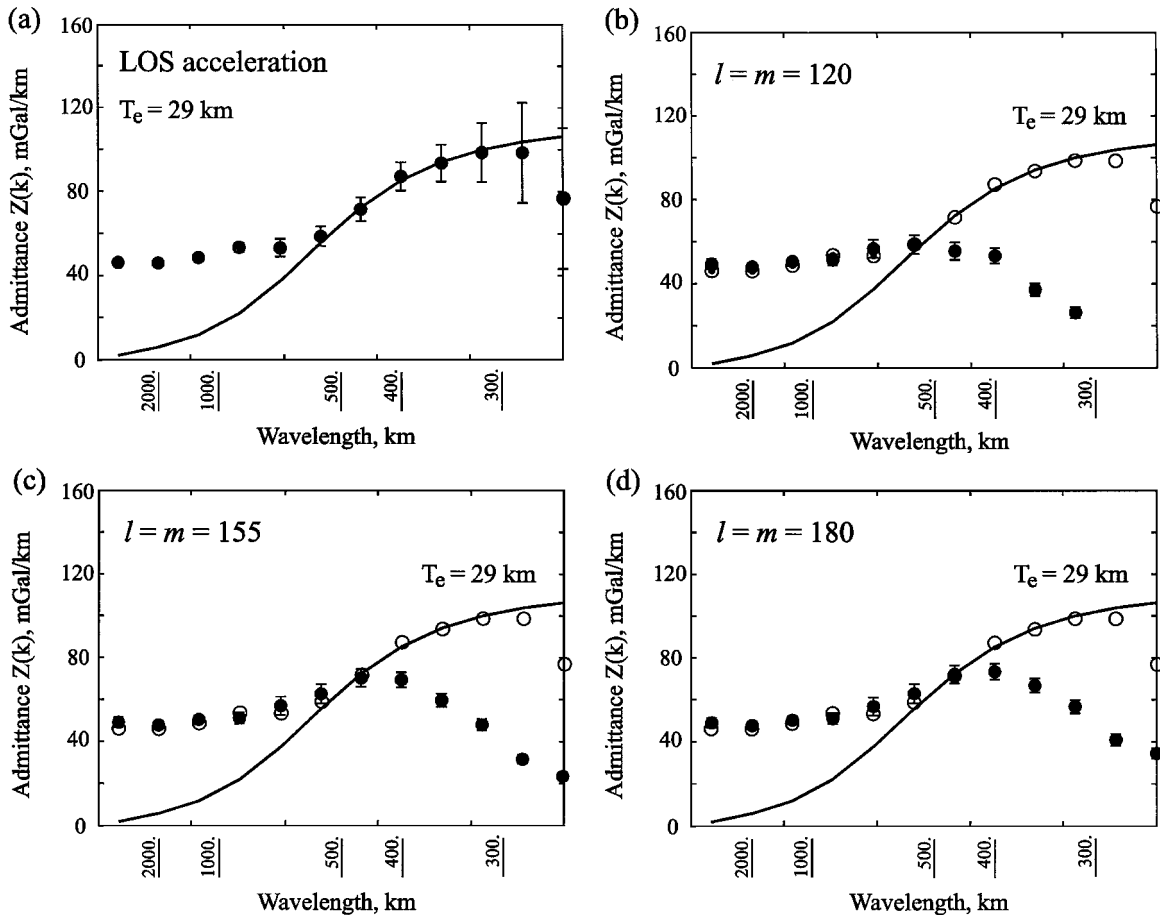


FIG. 7. Part (a) shows the calculated admittance values for Beta, as a function of wavelength, directly from the LOS accelerations. The solid line is the theoretical admittance curve for the best-fit elastic thickness to the data. Parts (b)–(d) show the admittance as a function of wavelength, calculated from three different spherical harmonic models of the gravity, to degree and order 120 (b), 155 (c), and 180 (d), and the gridded topography (solid dots). Shown for comparison on each plot are the admittance values calculated from the LOS accelerations (open circles) and the best-fit curve to these points, as in (a).

the width of the wavenumber bands, and the uncertainty in the admittance estimates. The value and position of the minimum of the misfit function is not dependent on Δk . The expression used to produce the theoretical admittance curves in this study (Eq. (2)) is calculated by approximating the elastic part of the lithosphere as a thin plane layer. Expressions for flexure of a thin spherical shell, similar to those given by Willemann and Turcotte (1982), change the estimates of T_e by a kilometer or less, because the radius of Venus is large compared with the size of the regions under consideration.

The results obtained here for Beta may also be compared with those produced from spherical harmonic representations of the gravity. Figure 7 shows admittance plots produced from gravity models to degree and order 120, 155, and 180. At wavelengths less than about 500 km, the admittance calculated from the spherical harmonics decreases, while that calculated from the LOS accelerations increases, so that at short wavelengths only the admittance estimates produced from the LOS accelerations give reliable estimates of the elastic thickness. The reason for the decrease with the spherical harmonics is likely to be the

low coherence between the observed Doppler derivative and the calculated LOS acceleration at wavelengths shorter than 500 km (see Figs. 8 and 9). The signal processing used in this work is effective because it extracts signals from the LOS accelerations which are coherent with those from the topography. However, the signal to noise ratio at short wavelengths is too low to allow the spherical harmonic gravity field itself to be accurately calculated. Note that, in moving from a model of degree and order 120 to ones of 155 and 180, there is some improvement in the calculated admittance values at wavelengths of around 500 km, but at shorter wavelengths the decrease to small admittance values is still observed.

4.2. Other Regions

Numerical estimates of T_e for the various other boxes are also shown in Table I. The values of T_e from cycle 4 obtained by McKenzie and Nimmo (1997) for their boxes are also shown, for comparison. Plots of the admittance, signal coherence, and misfit function are all shown in Figs. 8–15. In all cases, the

crustal thickness and density were assumed to be 16 km and 2670 kg m^{-3} , respectively. The values of T_e for the two “long-box” regions (Figs. 8–9) are well constrained, as the signal coherence in both cases remains high down to wavelengths as short as about 300 km, because the spacecraft altitude is relatively low. At longer wavelengths, the admittance spectra are fairly flat and

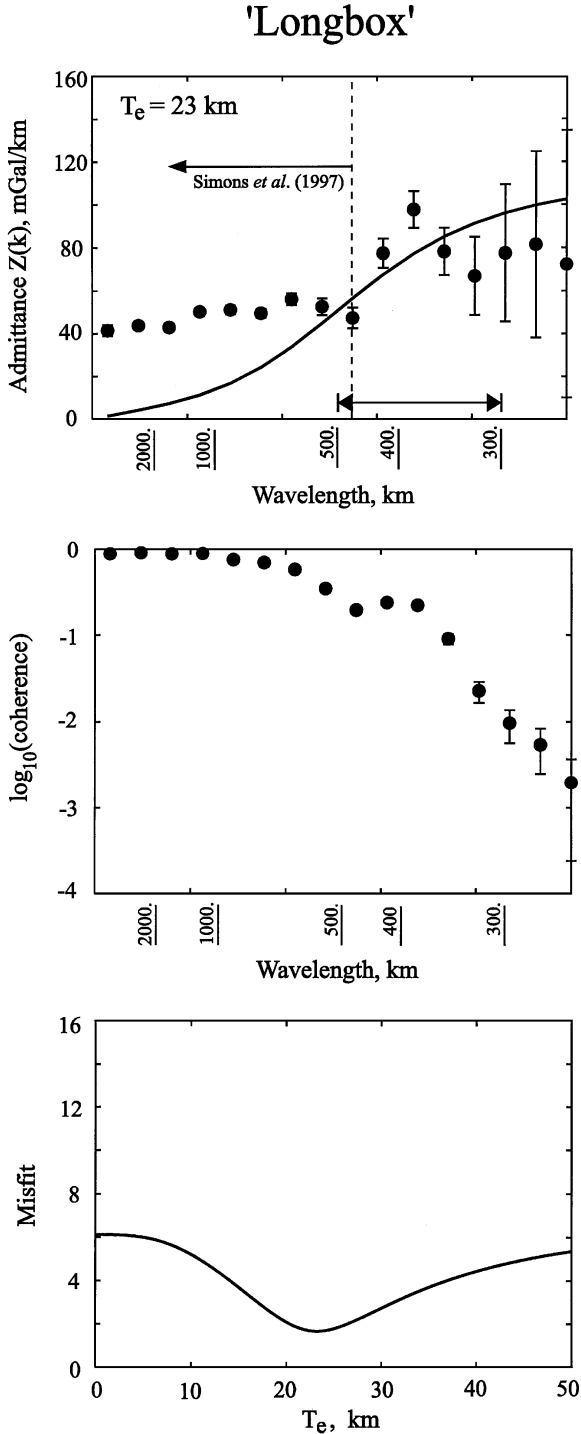


FIG. 8. As in Fig. 4, but for the “Longbox” region.

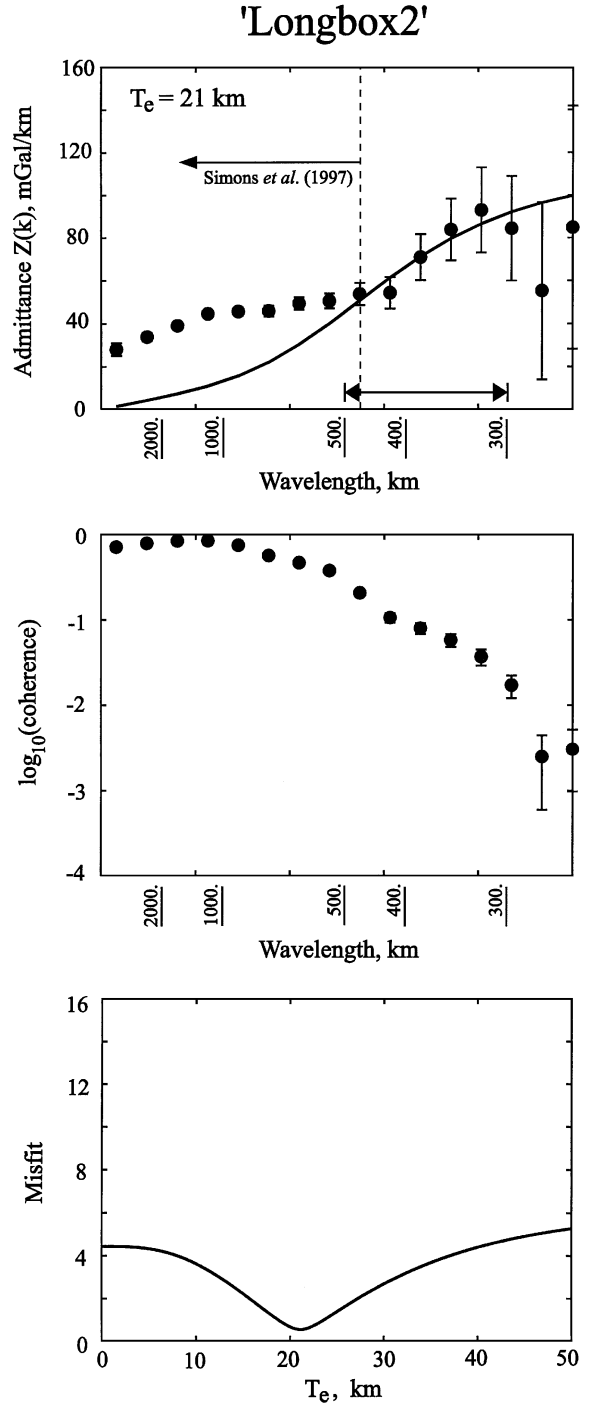


FIG. 9. As in Fig. 4, but for the “Longbox2” region.

have amplitudes of about 40 mGal km^{-1} , suggesting the long wavelength topography is convectively supported. Similarly, the estimate of T_e for Phoebe (Fig. 10) is fairly well constrained, because the altitude of the spacecraft is low and, as for Beta, the admittance values down to wavelengths of around 300 km are reliable. Note that the admittance is well determined and has a small uncertainty at wavelengths of about 350 km, although

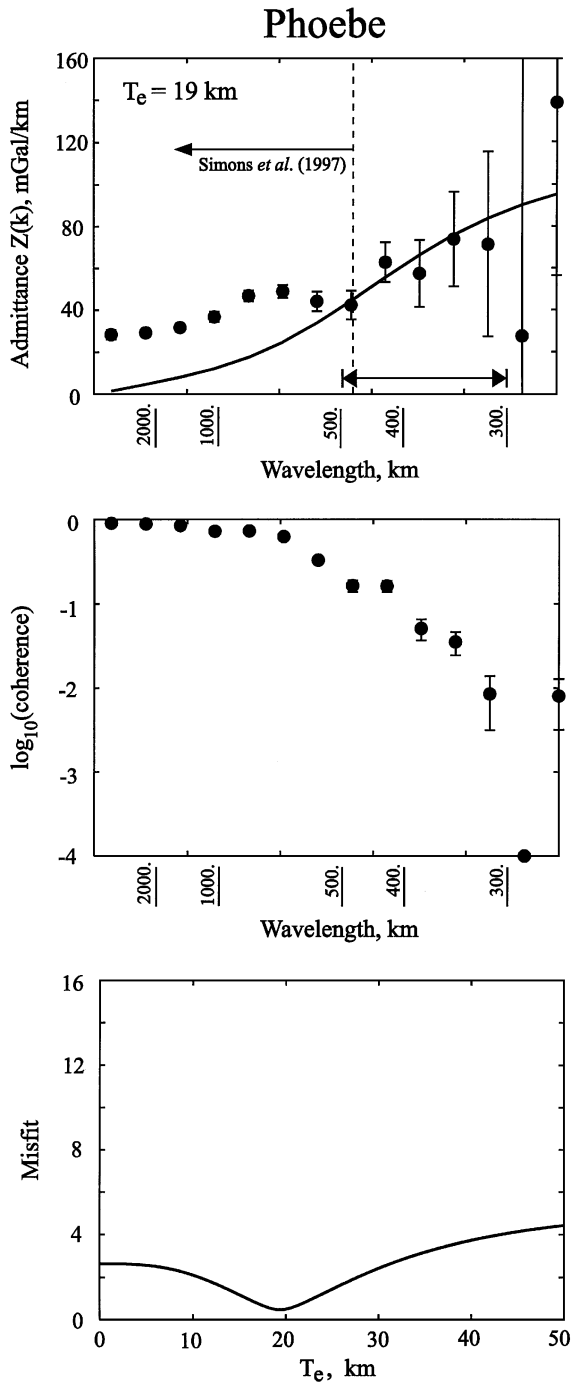


FIG. 10. As in Fig. 4, but for the Phoebe region.

the signal coherence is only of order 0.01. The value of T_e for Bell (Fig. 11) is, again, well constrained, as the signal coherence remains high down to rather short wavelengths (around 300 km). In the case of Eistla (Fig. 12), signal coherence is lost at longer wavelengths than for Bell, perhaps because the topography is less well determined, so the estimate of T_e is constrained by fewer points in the admittance plot.

The region south of Ovda (Fig. 13) maintains relatively high signal coherence down to wavelengths of around 350 km, and the estimate of T_e is again fairly well constrained. The estimate of T_e for the region of Ovda itself (Fig. 14) is not likely to be reliable, despite the high coherence at wavelengths as short as 350 km. The best-fit value of T_e within the wavelength band of 300–500 km is zero, and the plot of the misfit function suggests an upper limit of around 10 km. However, Ovda is a region of

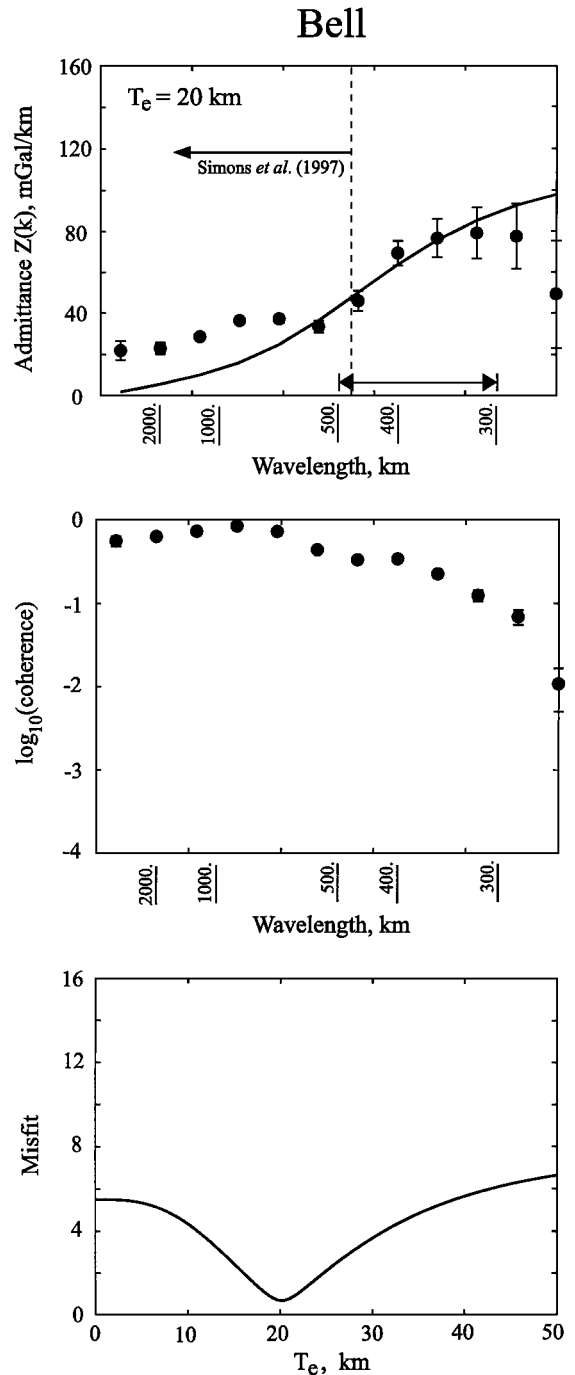


FIG. 11. As in Fig. 4, but for the Bell region.

Eistla

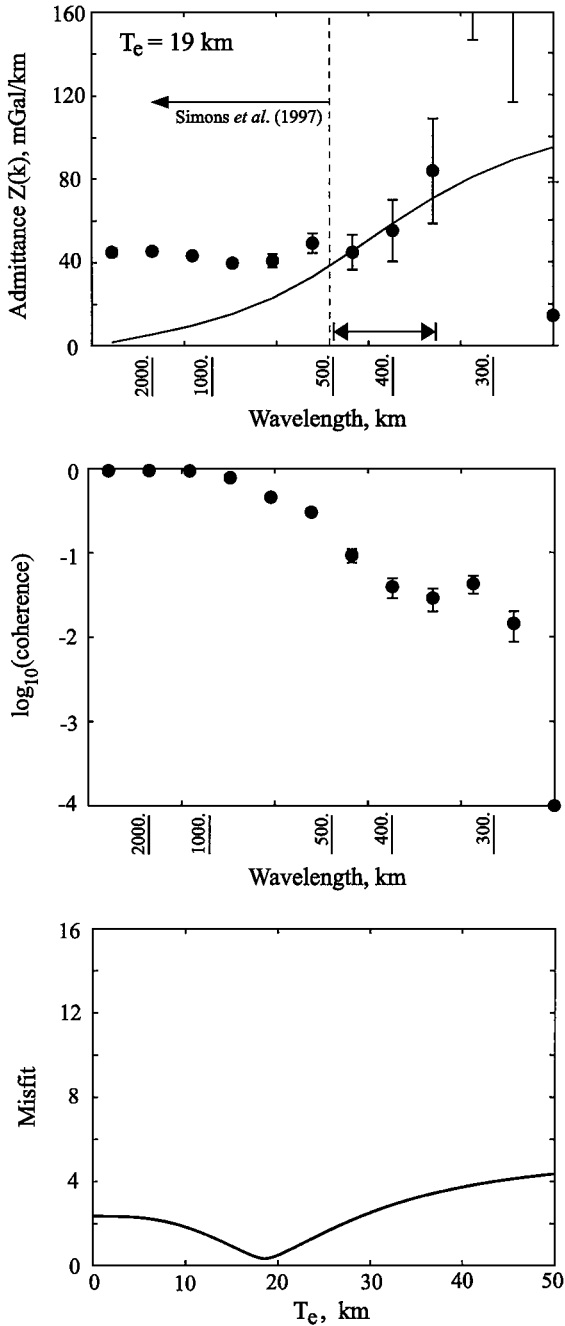


FIG. 12. As in Fig. 4, but for the Eistla region.

tessera terrain. Therefore, many of the best-fit picks for the point of the main radar echo are likely to be bad, and the topography is therefore poorly determined. If the noise is in the topography, the calculated admittance, Z' , will be reduced and is related to the true admittance, Z , by

$$Z' = \gamma^2 Z, \quad (5)$$

where γ is the coherence between the altimetry and the true topography (McKenzie 1994).

Much of the Alpha region (Fig. 15) is also tessera terrain, so the topography is poorly determined. The best-fit value of T_e suggested by the misfit function is again zero, but it is unlikely to be meaningful. In addition, signal coherence also drops off at

S of Ovda

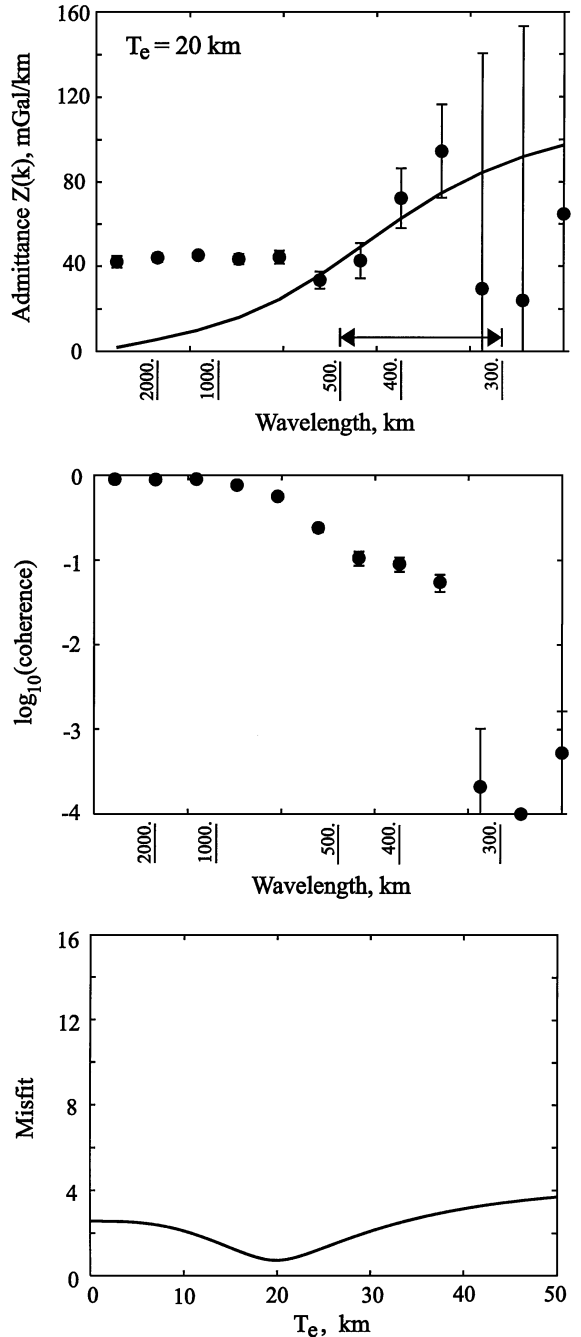


FIG. 13. As in Fig. 4, but for the South of Ovda region. Simons *et al.* (1997) made no study of this region.

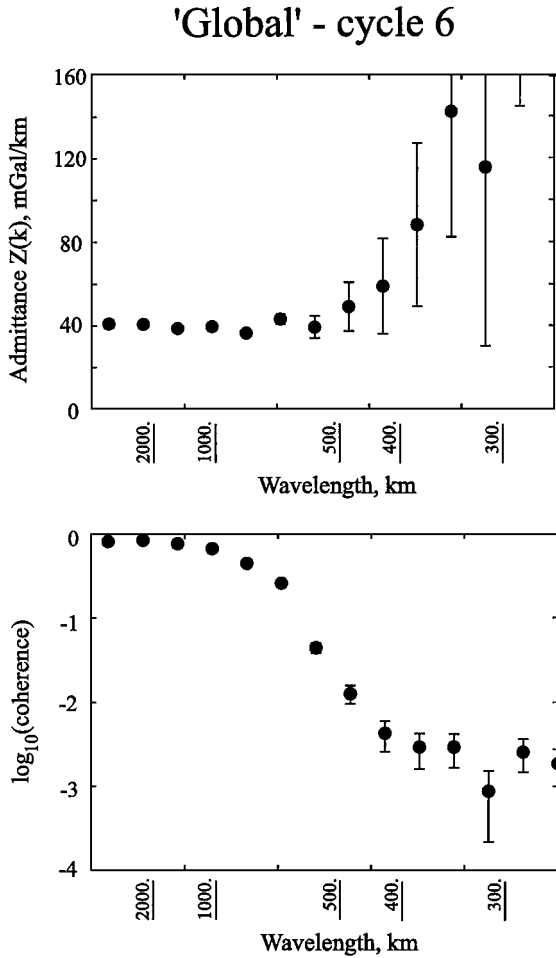


FIG. 16. Plots of admittance and signal coherence as a function of wavelength, using the cycle 6 data. No reliable estimate of T_e can be made from this data.

5. DISCUSSION AND CONCLUSIONS

The admittance curves can also be used to constrain crustal density and thickness, which were assumed constant in the previous section. These constraints will be illustrated by studying the data set for Beta, where the admittance estimates are well determined. For any given set of data, the best-fit value of T_e decreases if the assumed crustal density or thickness is increased. There is therefore a trade-off between the two, where a similar elastic thickness may be found if either a thin, dense crust or a thicker, lower density crust is assumed. The main constraint is that the crustal density at Beta must be less than about 3200 kg m^{-3} ; otherwise the predicted values of the admittance at short wavelengths are higher than the observed values (see Fig. 17). The best-fit value for the crustal density is around 2700 kg m^{-3} , although densities between 2400 and 3000 kg m^{-3} fit the observed data points within uncertainty. The constraint on crustal thickness is much weaker, because this parameter only affects the theoretical admittance curve at long wavelengths (see Fig. 18), where flexural effects are masked by the convective signature.

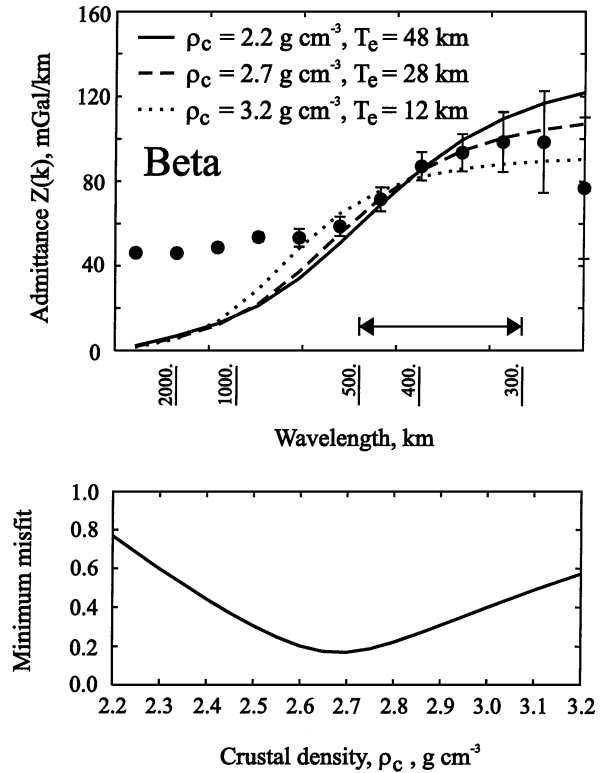


FIG. 17. The admittance plot for Beta as a function of wavelength. Fitted to the data points are a series of curves, which are the theoretical curves for the best-fit elastic thicknesses for the different values of crustal density given. In each case, the assumed crustal thickness is 16 km . The lower plot shows the value of the misfit function at its minimum (i.e., for the best-fit elastic thickness) as a function of crustal density.

In summary, though the admittance is affected by the crustal thickness and density, the regional variations in T_e found in this study are likely to result from real regional variations in the strength of the lithosphere. If, for instance, the elastic thickness of Beta were the same as that for Bell (with the latter having a

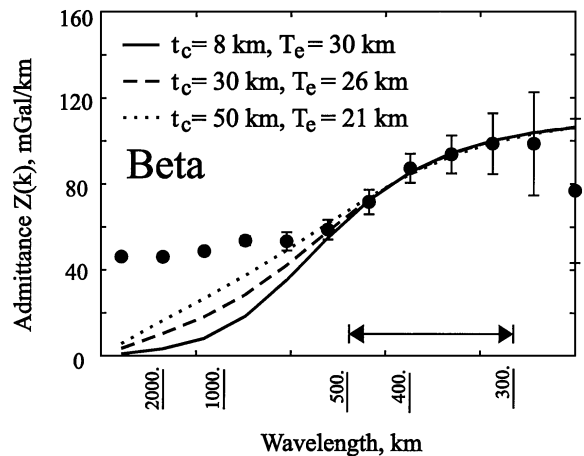


FIG. 18. As in Fig. 16, but with the crustal density assumed to be 2670 kg m^{-3} , to show the effects of varying the assumed crustal thickness.

crustal thickness of 16 km and a density of 2670 kg m^{-3}), the crustal density of Beta would have to exceed 2900 kg m^{-3} , unless the crustal thickness exceeded about 25 km. Even for a crustal thickness of 30 km, a crustal density of around 2850 kg m^{-3} would be necessary for the best-fit elastic thickness of Beta to be as small as that for Bell. These high crustal densities produce poorer fits to the data, as shown by the misfit function (see Fig. 17). It is therefore reasonable to conclude that there are regional variations in elastic thickness between different areas of Venus.

The assumed values for the crustal parameters in this study are those used by McKenzie and Nimmo (1997), to aid comparison of results. The value of 2670 kg m^{-3} for crustal density is the standard value used for Bouguer corrections on Earth and has been well constrained by short wavelength admittance values in terrestrial studies (see, e.g., McKenzie and Fairhead 1997). There is some suggestion that the highland plateau regions of Venus such as Ovda are isostatically compensated by thicker crust than elsewhere (e.g., Kucinskas and Turcotte 1994, Moore and Schubert 1997, Simons *et al.* 1997), but in these regions, the topography is too poorly determined at all wavelengths shorter than about 1000 km for the admittance estimates calculated in this work to be reliable.

The results obtained by Johnson and Sandwell (1994) (see Fig. 3) by flexural modeling of large features show elastic thicknesses similar to those found in this study. Those values found by modeling smaller features seem to be systematically lower, but the amplitudes of the topographic signals used are small and sometimes vary markedly from one orbit to the next. In addition, McGovern and Solomon (1998) remark that elastic thickness estimates at coronae tend, in general, to be somewhat lower than estimates made elsewhere. They suggest that coronae are the surface expressions of mantle upwellings beneath weak lithosphere, upwellings beneath stronger lithosphere giving rise to large volcanoes. They argue that coronae tend, on average, to be older than shield volcanoes, assuming that the lithospheric thickness of Venus (and hence T_e) has been increasing with time.

The values obtained in this work show evidence of regional variations in T_e , between about 19 and 29 km, for areas where the topography is reliable. This variability is likely to be real, rather than the result of errors in the estimates of T_e . The main trends are consistent with those found by McKenzie and Nimmo (1997), where such comparisons are possible, although the range of values found in this study was smaller. For example, both studies found a smaller elastic thickness for Eistla than for the region containing Beta and Phoebe. Over the region studied, the mean effective elastic thickness is between 21 and 23 km, also in agreement with previous studies (e.g., Simons *et al.* 1997). The elastic thickness values determined for Venus are similar to those observed in shields and old ocean basins on Earth. The surface temperature of Venus (around 450°C) is much higher than that of the Earth and is approximately the temperature which marks the base of the elastic part of the lithosphere on Earth (Watts 1994). This difference is consistent with the lithosphere of Venus

being dry, and thus able to withstand elastic stresses at higher temperatures than terrestrial lithosphere (see, e.g., Nimmo and McKenzie (1998)). Also, the surface heat flux on Venus must be smaller than that of the Earth if the temperature at around 20 km depth is to be low enough for the plate to behave elastically. The magnitude of the variations in elastic thickness observed in this study are close to the limit of resolution of this method. However, the implication of regional variations in T_e is that there are also regional variations in the thickness of the venusian lithosphere.

Simons *et al.* (1997) have also used the gravity field of Venus to estimate the elastic thickness of the lithosphere, but they used a different approach from that of McKenzie and Nimmo (1997) and that used here. The most important difference is that Simons *et al.* used the spherical harmonic coefficients of the gravity field, determined from the orbits of Magellan and Pioneer Venus, which are tabulated to $l = m = 120$. Simons *et al.* state that the admittance estimate at some degree l is sensitive to gravity coefficients in the range $l \pm l_{\text{window}}$, where l_{window} is the maximum degree in the spherical harmonic representation of the window for the data. For each area studied, an estimate was made of the maximum degree, l_{obs} , which was resolved in the harmonic model, and from this a corresponding value of l_{nyq} (≤ 80) was calculated, where $l_{\text{nyq}} = l_{\text{obs}} - l_{\text{window}}$. The admittance estimate centered at l_{nyq} therefore contains information up to degree l_{obs} . Simons *et al.* claim that this approach allows short wavelength information to be used to constrain the value of T_e . However, the spherical harmonic coefficients at wavelengths corresponding to $l > l_{\text{nyq}}$ are systematically too small, as shown by the comparison between the admittance estimates for Beta calculated from the LOS accelerations and those from the spherical harmonic gravity coefficients, in Fig. 7. The reason the gravity field at wavelengths shorter than about 500 km cannot reliably be determined from the orbital data is that the surface gravity field is reduced by a factor of about 20 at the height of the satellite, because of upward attenuation. The resulting Doppler signal is then less than the noise.

The method employed in this study involves projection of the LOS accelerations onto a plane, which results in distortion at wavelengths comparable to the radius of Venus. Simons *et al.* use the topography to estimate the admittance, Z , and its uncertainty by a method that uses a spherical harmonic representation of an axisymmetric smooth window. Their method therefore avoids the distortions that arise from projection onto a plane. However, this distortion is unimportant, since for elastic thicknesses of order 20 km, it is at wavelengths shorter than around 500 km that the theoretical admittance profiles must be constrained by the data to allow estimation of T_e (see below). At these wavelengths, distortion is small. An advantage of the method described here is that it enables us to use the multitaper technique, which greatly reduces spectral leakage. A disadvantage of Simons *et al.*'s approach is that their estimates of the uncertainty in Z at different values of l are not independent.

A more important problem arises from Simons *et al.*'s inability to use wavelengths shorter than about 500 km, since it is at

these wavelengths that the influence of elasticity is most obvious and causes the admittance to increase from its long wavelength value of around 20–50 mGal km⁻¹. At longer wavelengths, the effects of convective support are important, and it is not possible to separate the effects of convection and elastic flexure using only gravity and topography. For this reason, in this study no admittance estimates produced from gravity signals with wavelengths longer than about 500 km are used to estimate T_e . Reliable admittance estimates can be obtained at wavelengths as short as 250 km when the signal to noise ratio is as low as 0.01, because only that part of the LOS acceleration which is coherent with the topography is extracted by the signal processing.

The long wavelength topography and gravity associated with Beta, Phoebe, Bell, and Eistla are suspected to be convective in origin, not only because of the presence of roughly circular, positive gravity and topography anomalies but also because the long wavelength admittance spectra are flat, with amplitudes between about 20 and 50 mGal km⁻¹, in agreement with the values predicted by convective modeling. There is also evidence of rifting and volcanic constructs in the SAR images. In general, the form of the admittance spectra suggests that the long wavelength topography of Venus is dynamically supported, a conclusion which is supported by Simons *et al.* (1997).

Another major conclusion of this work is the importance of the altitude of the spacecraft when studying gravitational signals in the wavelength range necessary to investigate elastic effects. If the altitude is too high, signal attenuation makes admittance studies unreliable. This effect prevents reliable estimates of T_e from being obtained from cycle 6, where the spacecraft altitude varied in the range 250 to 450 km, approximately, and from about half of cycle 5.

ACKNOWLEDGMENTS

We thank Jim Alexopoulos and James McKenzie for their help, and Mark Simons and Algis Kucinskas for their reviews. This work was carried out with the support of Schlumberger Cambridge Research, the Newton Trust, Magdalene College, and grants from the Royal Society and NERC. Department of Earth Sciences, Cambridge University, contribution number 5881.

REFERENCES

- Brown, C. D., and R. E. Grimm 1996. Floor subsidence and rebound of large Venus craters. *J. Geophys. Res.* **101**, 26057–26067.
- Ford, J. P., J. J. Plaut, C. M. Weitz, T. G. Farr, D. A. Senske, E. R. Stofan, G. Michaels, and T. J. Parker 1993. Guide to Magellan image interpretation. Jet Propulsion Laboratory publication 93-24.
- Johnson, C. L., and D. T. Sandwell 1994. Lithospheric flexure on Venus. *Geophys. J. Int.* **119**, 627–647.
- Konopliv, A. S., and W. L. Sjogren 1996. Venus gravity handbook. Jet Propulsion Laboratory publication 96-2.
- Kucinskas, A. B., and D. L. Turcotte 1994. Isostatic compensation of equatorial highlands on Venus. *Icarus* **112**, 104–116.
- McGill, G. E., S. J. Steenstrup, C. Barton, and P. G. Ford 1981. Continental rifting and the origin of Beta Regio, Venus. *Geophys. Res. Lett.* **8**, 737–740.
- McGovern, P. J., and S. C. Solomon 1998. Growth of large volcanoes on Venus: Mechanical models and implications for structural evolution. *J. Geophys. Res.* **103**, 11071–11101.
- McKenzie, D. 1994. The relationship between topography and gravity on Earth and Venus. *Icarus* **112**, 55–88.
- McKenzie, D., and C. Bowin 1976. The relationship between bathymetry and gravity in the Atlantic Ocean. *J. Geophys. Res.* **81**, 1903–1915.
- McKenzie, D., and D. Fairhead 1997. Estimates of the effective elastic thickness of the continental lithosphere from Bouguer and free air gravity anomalies. *J. Geophys. Res.* **102**, 27523–27552.
- McKenzie, D., and F. Nimmo 1997. Elastic thickness estimates for Venus from line of sight accelerations. *Icarus* **130**, 198–216.
- Moore, W. B., and G. Schubert 1997. Venusian crustal and lithospheric properties from nonlinear regressions of highland geoid and topography. *Icarus* **128**, 415–428.
- Nimmo, F., and D. McKenzie 1996. Modelling plume-related uplift, gravity and melting on Venus. *Earth Planet. Sci. Lett.* **145**, 109–123.
- Nimmo, F., and D. McKenzie 1998. Volcanism and tectonics on Venus. *Annu. Rev. Earth Planet. Sci.* **26**, 23–51.
- Phillips, R. J. 1994. Estimating lithospheric properties at Atla Regio, Venus. *Icarus* **112**, 147–170.
- Phillips, R. J., W. M. Kaula, G. E. McGill, and M. C. Malin 1981. Tectonics and evolution of Venus. *Science* **212**, 879–887.
- Phillips, R. J., C. L. Johnson, S. J. Mackwell, P. Morgan, D. T. Sandwell, and M. T. Zuber 1997. Lithospheric mechanics and dynamics of Venus. In *Venus II* (S. W. Bougher, D. M. Hunten, and R. J. Phillips, Eds.), pp. 1163–1204. Univ. of Arizona Press, Tucson.
- Rappaport, N. J., and J. J. Plaut 1994. 360 degree and order model of venusian topography. *Icarus* **112**, 27–33.
- Rappaport, N. J., A. S. Konopliv, and A. B. Kucinskas 1999. An improved 360 degree and order model of Venus topography. *Icarus* **139**, 19–31.
- Ricard, Y., L. Fleitout, and C. Froidevaux 1984. Geoid heights and lithospheric stresses for a dynamic Earth. *Ann. Geophysicae* **2**, 267–286.
- Richards, M. A., and B. H. Hager 1984. Geoid anomalies in a dynamic Earth. *J. Geophys. Res.* **89**, 5987–6002.
- Saunders, R. S., A. J. Spear, P. C. Allin, R. S. Austin, A. L. Berman, R. C. Chandlee, J. Clark, A. V. deCharon, E. M. De Jong, D. G. Griffith, J. M. Gunn, S. Hensley, W. T. K. Johnson, C. E. Kirby, K. S. Leung, D. T. Lyons, G. A. Michaels, J. Miller, R. B. Morris, A. D. Morrison, R. G. Piereson, J. F. Scott, S. J. Schaffer, J. P. Slonski, E. R. Stofan, T. W. Thompson, and S. D. Wall 1992. Magellan mission summary. *J. Geophys. Res.* **97**, 13067–13091.
- Simons, M., S. C. Solomon, and B. H. Hager 1997. Localization of gravity and topography: Constraints on the tectonics and mantle dynamics of Venus. *Geophys. J. Int.* **131**, 24–44.
- Smrekar, S. E. 1994. Evidence for active hotspots on Venus from analysis of Magellan gravity data. *Icarus* **112**, 2–26.
- Snyder, J. P. 1989. An album of map projections. USGS Professional Paper 1453.
- Thomson, D. J. 1982. Spectrum estimation and harmonic analysis. *Proc. IEEE* **70**, 1055–1096.
- Watts, A. B. 1994. Crustal structure, gravity anomalies and flexure of the lithosphere in the vicinity of the Canary Islands. *Geophys. J. Int.* **119**, 648–666.
- Willemann, R. J., and D. L. Turcotte 1982. The role of lithospheric stress in the support of the Tharsis Rise. *J. Geophys. Res.* **87**, 9793–9801.